Supporting Information

Photo-oligomerization by shifting the coordination site in a luminescent coordination polymer

Wei-Chao Song,[†] Chen-Chen Geng,[†] Sheng-Yang Li,[†] Ling Liang,[†] Xiu-Guang Wang,[†] En-Cui Yang,*[,†] and Xiao-Jun Zhao*[,†,‡]

[†]College of Chemistry, Tianjin Key Laboratory of Structure and Performance for Functional Molecules, Tianjin Normal University, Tianjin 300387, China

[‡]Collaborative Innovation Center of Chemical Science and Engineering (Tianjin), Tianjin 300071, China

Table of Contents

General procedures. --S3

Preparation of 1,4-Bis(β-pyrazinyl-2-vinyl)-benzene (bpzvb) --S3

Synthesis of [Zn(bpzvb)(ip)]$_n$ (1) --S3

Synthesis of irradiated sample 1a --S3

Synthesis of irradiated powder sample 1-UV-t --S4

Conversion from 1-UV-2h to 1 --S4

Isolation of the oligomer --S4

X-ray Crystallography --S4

Table S1. Summary of the distances for intraligand and interligand pairs --S5

Table S2. Crystal data and structure refinement for complexes **1** and **1a** --S5

Table S3. Selected bond lengths (Å) and angles (°) for complexes **1** and **1a** --S6

Scheme S1. Five possible photo-oligomerization products of bpzvb [2+2] cycloadditions--S7

Fig. S1. The prototype of experimentally known examples --S8

Fig. S2. PXRD patterns of complex **1** upon UV light, and treatment with heat --S9

Fig. S3. Thermogravimetric analysis and differential calorimetry of **1** and **1a** --S9

Fig. S4. PXRD patterns of powdered **1a** upon treatment with heat --S10

Fig. S5. Raman spectra for the complexes **1** and **1a** --S10

Fig. S6. ^{1}H NMR spectra of **1** in $CDCl_3$ plotted at different UV irradiation times --S11

Fig. S7. ^{1}H NMR (400 MHz) of pbzvb --S12

Fig. S8. ^{1}H NMR (400 MHz) of the dimer-I --S13

Fig. S9. ^{1}H NMR (400 MHz) of the trimer --S14

Fig. S10. ^{1}H NMR (400 MHz) of the tetramer --S15

Fig. S11. NOESY of dimer-I --S16

Fig. S12. The characteristic proton peaks of oligomers --S16

Fig. S13. The trajectory of the CIE color coordinates during the phase transitions of **1** to **1a** --S17

Fig. S14. ^{1}H NMR spectra of **1-UV-2h** upon treatment with heat--S17

References--S18

General procedure. All raw reagents were commercially available without further purification. PXRD patterns were measured on a Bruker D8 ADVANCE diffractometer at 40 kV, 40 mA for Cu Kα radiation (λ = 1.5406 Å). Simulation of the PXRD pattern was carried out by the single-crystal data and diffraction-crystal module of the Mercury (Hg) program version 3.0. FT-IR (KBr pellets) spectra were carried out on a Nicolet Avatar-370 spectrometer in the range 4000 - 400 cm^{-1}. TG/DSC were carried out in a NETZSCH STA 449 F5 instrument under N_2 atmosphere at a heating rate of 10 ºC min^{-1}. Elemental analyses for C, H, and N were recorded on a Perkin-Elmer 2400C elemental analyzer. FT-Raman measurements were carried out using a Nicolet iS50, in which the Raman laser power is 0.05 W. ^1H NMR and 2D NOESY spectra were measured on Bruker-400 spectrometer (400 MHz). Chemical shifts were reported in ppm using tetramethylsilane (TMS) as the internal standard. NMR samples were dissolved n $CDCl_3$. Mass spectrometry analyses were performed on an Agilent 6500 series quadrupole time-of-flight (QTOF) mass spectrometer, operating in the positive ion mode. Fluorescence spectra of the solid samples were collected on Horiba Jobin Yvon Flurolog-3 at room temperature.

Preparation of 1,4-Bis(β-pyrazinyl-2-vinyl)-benzene (bpzvb): The bpzvb ligand was synthesized according to the literature method.[S1]

Synthesis of [Zn(bpzvb)(ip)]*n* (1). Bpzvb (14.3 mg, 0.05 mmol), isophthalic acid (H_2ip, 8.3 mg, 0.05 mmol), $Zn(NO_3)_2 \cdot 6H_2O$ (14.9 mg, 0.05 mmol), water (3.0 mL), and NaOH (4.0 mg, 0.1 mmol) were suspended in a 23.0 mL Teflon reactor. The reactor was heated at 160 ºC for 4 days under autogeneous pressure. After the mixture was cooled to room temperature at 6 ºC h^{-1}, yellow block-shape single crystals of **1** were obtained directly (Yield: 30% based on bpzvb). Anal. Calcd for $C_{26}H_{18}N_4O_4Zn$: C, 60.54%; H, 3.52%; N, 10.86%. Found: C, 60.12%; H, 3.33%; N, 10.66%. FT-IR (KBr, cm^{-1}): 3058 (w), 1613 (s), 1577 (m), 1552 (m), 1516 (m), 1452 (m), 1399 (s), 1298 (w), 1141 (w), 1071 (w), 1015 (w), 967 (w), 847 (w), 743 (m), 722 (m), 661(w) , 573(w).

Synthesis of irradiated sample 1a. Single crystals of **1** were directly irradiated by a 400 W Hg lamp for 24 h, leading to yellow block-shaped single crystals of **1a**. Anal. Calcd for $C_{26}H_{18}N_4O_4Zn$: C, 60.54%; H, 3.52%; N, 10.86%. Found: C, 60.25%; H, 3.44%; N, 10.75%. FT-IR (KBr, cm^{-1}): 3057 (w), 1612 (s), 1575(s), 1553 (s), 1518 (w), 1452 (m), 1389 (s), 1302 (w), 1152 (w), 1071 (w), 1017 (w), 975 (w), 916 (w), 833 (w), 742 (m), 724 (m).

Synthesis of irradiated powder sample 1-UV-t. Single crystals of **1a** (20 mg) were finely ground and dispersed in 2 mL of cyclohexane with stirring and irradiated for a specific time with a 400 W high-pressure mercury lamp at room temperature. The product was collected and dried in vacuo at room temperature.

Conversion from 1-UV-2h to 1. The powder sample **1-UV-2h** was heated at 250 ºC for 3 h.

Isolation of the oligomer. The obtained powder was transferred to a 10 mL bottle with 4 mL of $NH_3{\cdot}H_2O$, shaken at ambient conditions for 2 hours. The precipitate was filtered and washed with water, then dried in vacuo at room temperature. The crude product was purified by column chromatography using silica as the stationary phase and CH_2Cl_2 : CH_3OH = 20 : 1 as the eluent.

X-ray Crystallography. Diffraction intensities were collected on a Bruker APEX-II QUAZAR diffractometer at 173 K for **1** by using the φ-ω scan technique and Mo-Kα radiation (λ = 0.71073 Å). Single-crystal X-ray diffraction data for **1a** were collected on a SuperNova, Dual, Cu at home/near, AtlasS2 diffractometer (λ = 1.5418 Å) at 293 K. The structures were solved by the direct methods and refined by full-matrix least-squares refinements based on *F*2 with the SHELXTL program.[S2-S3] The non-H atoms were located by difference Fourier maps and subjected to anisotropic refinement. Hydrogen atoms were added according to the theoretical models. The summary of crystallographic data for the complexes was listed in Table S2, and the selected bond lengths and angles were given in Table S3.

Table S1. Summary of the distances for intraligand and interligand pairs

CCDC	ligand	Distance/ Å	
		intraligand pair	interligand pair
1585076	1,4-bis[2-(4-pyridyl)ethenyl]benzene (bpeb)[S4]	3.744	7.500
786146	N,N′-bis(4-pyridinecarboxamide)-4-benzene (4-bpcb)[S5]	4.062	7.043
777807	N,N′-bis(3-pyridinecarboxamide)-1,4-benzene(3-bpcb)[S5]	3.996	4.105
1901823	1,4-bis(β-pyrazinyl-2-vinyl)-benzene (bpzvb, present work)	3.834	3.831

Table S2. Crystal data and structure refinement for the CPs [a]

	1	**1a**
Chemical formula	$C_{26}H_{18}N_4O_4Zn$	$C_{26}H_{18}N_4O_4Zn$
F_w	515.81	515.81
T (K)	173(2)	293(2)
Cryst syst	Triclinic	Triclinic
Space group	$P\overline{1}$	$P\overline{1}$
a (Å)	7.7964(3)	8.2190(4)
b (Å)	10.0946(4)	10.0622(5)
c (Å)	14.0983(6)	13.9221(7)
α	88.0480(10)	89.079(4)
β (deg)	79.5450(10)	76.966(4)
γ	76.4250(10)	76.522(4)
V (Å^3)	1060.61(7)	1090.0(1)
Z	2	2
D_c (g cm^{-3})	1.615	1.572
$F(000)$	528	528
μ (mm^{-1})	1.203	1.935
Reflections collected / unique	7934 / 5225	6957 / 3879
R_{int}	0.0151	0.0694
R_1 [a], wR_2 [b] [$I > 2\sigma(I)$]	0.0266 / 0.0687	0.0698 / 0.1695
R_1, wR_2 [all data]	0.0289 / 0.0699	0.0969 / 0.1878
GOF on F^2	1.055	1.035
$\Delta\rho_{max}$, $\Delta\rho_{min}$ / e·Å^{-3}	0.491, −0.290	2.05, −0.41

[a] $R_1 = \Sigma||F_o||F_c||/|F_o|$. [b] $wR_2 = [\Sigma w(|F_o^2|-|F_c^2|)^2/\Sigma w(|F_o^2|)^2]^{1/2}$

Table S3. Selected bond lengths (Å) and angles (°) for **1** and **1a** [a]

	1		
Zn(1)–O(1)	2.0244(10)	Zn(1)–O(2)$^{\#1}$	2.0502(10)
Zn(1)–N(3)$^{\#3}$	2.1640(13)	Zn(1)–N(1)	2.1874(13)
Zn(1)–O(4)$^{\#2}$	2.2232(11)	Zn(1)–O(3)$^{\#2}$	2.1540(11)
O(1)–Zn(1)–O(2$^{)\#1}$	113.96(4)	N(1)–Zn(1)–O(4)$^{\#2}$	88.59(5)
O(2)$^{\#1}$–Zn(1)–O(3)$^{\#2}$	92.55(4)	O(1)–Zn(1)–N(3)$^{\#3}$	95.41(5)
O(2)$^{\#1}$–Zn(1)–N(3)$^{\#3}$	90.28(4)	O(3)$^{\#2}$–Zn(1)–N(3)$^{\#3}$	88.72(5)
O(1)–Zn(1)–N(1)	87.65(5)	O(2)$^{\#1}$–Zn(1)–N(1)	83.46(4)
O(3)$^{\#2}$–Zn(1)–N(1)	91.02(5)	O(1)–Zn(1)–O(4)$^{\#2}$	92.75(4)
O(3)$^{\#2}$–Zn(1)–O(4)$^{\#2}$	60.34(4)	N(3)$^{\#3}$–Zn(1)–O(4)$^{\#2}$	96.73(5)
	1a		
Zn(1)–O(4)	2.220(4)	Zn(1)–O(3)	2.145(4)
Zn(1)$^{\#1}$–O(2)	2.044(3)	Zn(1)$^{\#2}$–O(1)	2.024(3)
Zn(1)–N(3B)	2.287(19)	Zn(1)–N(1A)$^{\#3}$	2.15(3)
O(4)–Zn(1)–N(3$^{)}$	95.8(7)	O(1)$^{\#4}$–Zn(1)–O(4)	93.33(14)
O(3)–Zn(1)–O(4)	59.37(14)	O(1)$^{\#4}$–Zn(1)–O(3)	152.69(15)
O(3)–Zn(1)–N(3B)	92.5(6)	O(1)$^{\#4}$–Zn(1)–O(2)$^{\#1}$	115.50(14)
O(3)–Zn(1)–N(1A)$^{\#3}$	92.1(11)	O(1)$^{\#4}$–Zn(1)–N(3B)	91.0(5)
O(2)$^{\#1}$–Zn(1)–O(4)	150.46(14)	O(1)$^{\#4}$–Zn(1)–N(1A)$^{\#3}$	86.9(9)
O(2)$^{\#1}$–Zn(1)–O(3)	91.57(14)	N(1A)$^{\#3}$–Zn(1)–O(4)	90.2(13)
O(2)$^{\#1}$–Zn(1)–N(3B)	90.3(7)	N(1A)$^{\#3}$–Zn(1)–N(3B)	173.8(14)
O(2)$^{\#1}$–Zn(1)–N(1A)$^{\#3}$	85.4(12)		

[a] Symmetry codes for **1**: $^{\#1}$ - x + 2, - y + 1, - z; $^{\#2}$ x, y - 1, z; $^{\#3}$ x + 1, y - 1, z - 1. Symmetry codes for **1a**: $^{\#1}$ - x + 1, - y + 2, - z + 3; $^{\#2}$ x, y - 1, z; $^{\#3}$ - x + 1, - y + 3, - z + 3; $^{\#4}$ x, y + 1, z; $^{\#5}$ - x + 2, - y + 1, - z + 2.

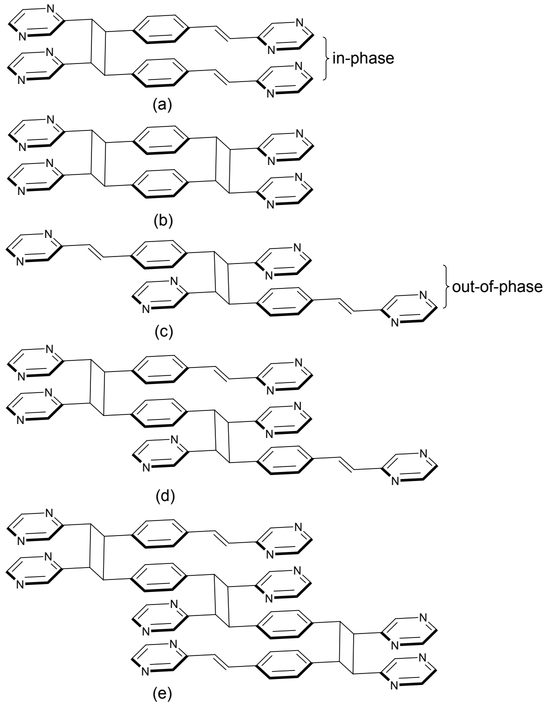

Scheme S1. Five possible photo-oligomerization products of bpzvb [2+2] cycloadditions: dimer-I (a), dimer-II (b), dimer-III (c), trimer (d), and tetramer (e).

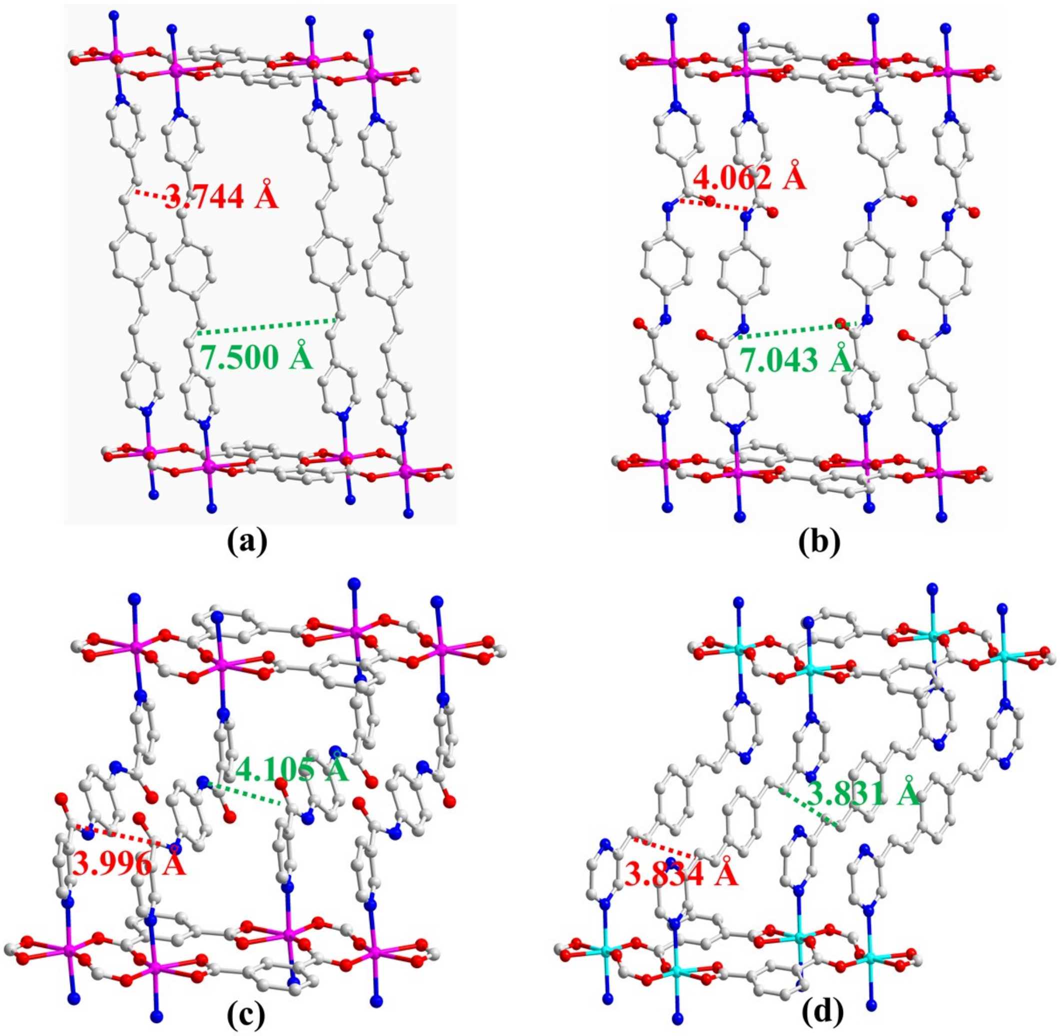

Fig. S1. The prototype of experimentally known examples. (a) [Co(bpeb)(isophthalic)]·1.5DMA (CCDC 1585076);[S4] (b) [Co(4-bpcb)(1,3-BDC)]·$2H_2O$ (CCDC 786146);[S5] (c) [Co(3-bpcb)(1,3-BDC)]·H_2O (CCDC 777807);[S5] (d) $[Zn(bpzvb)(ip)]_n$ (CCDC 1901823), the present work. 1,3-benzenedicarboxylate/isophthalic acid (1,3-H_2BDC).

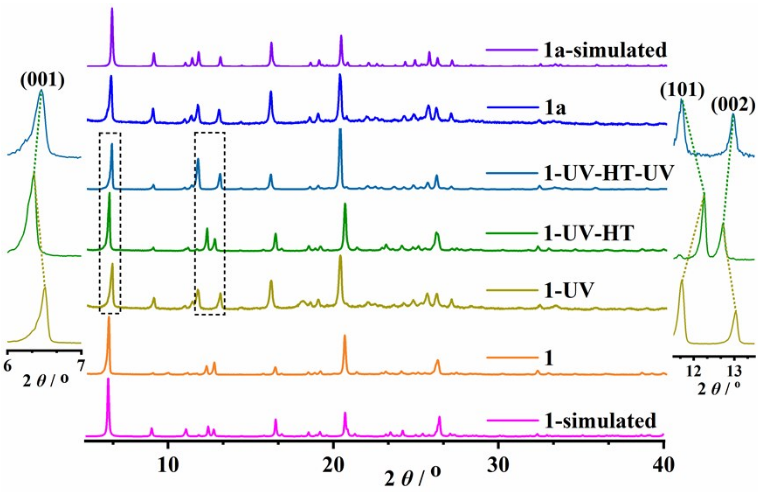

Fig. S2. PXRD patterns of complex **1** upon UV light, and treatment with heat.

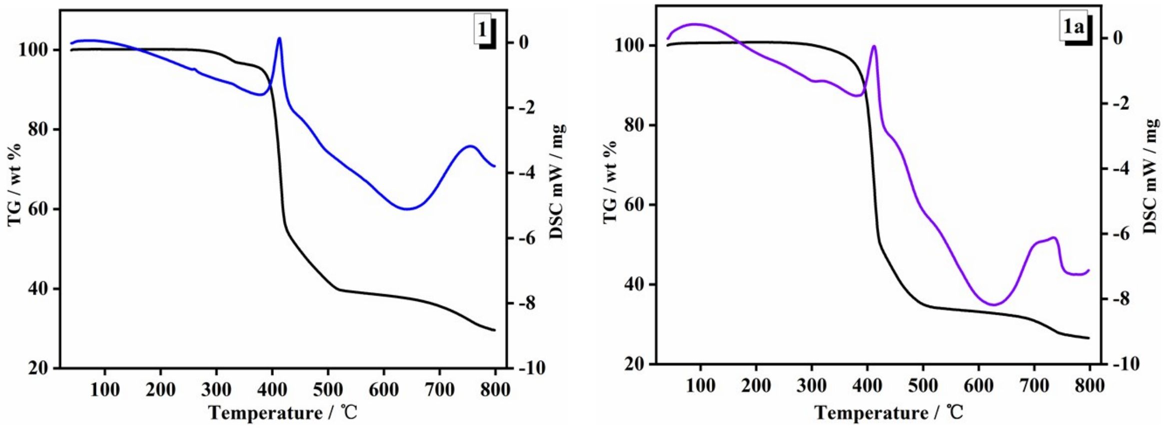

Fig. S3. Thermogravimetric analysis and differential calorimetry of **1** and **1a**.

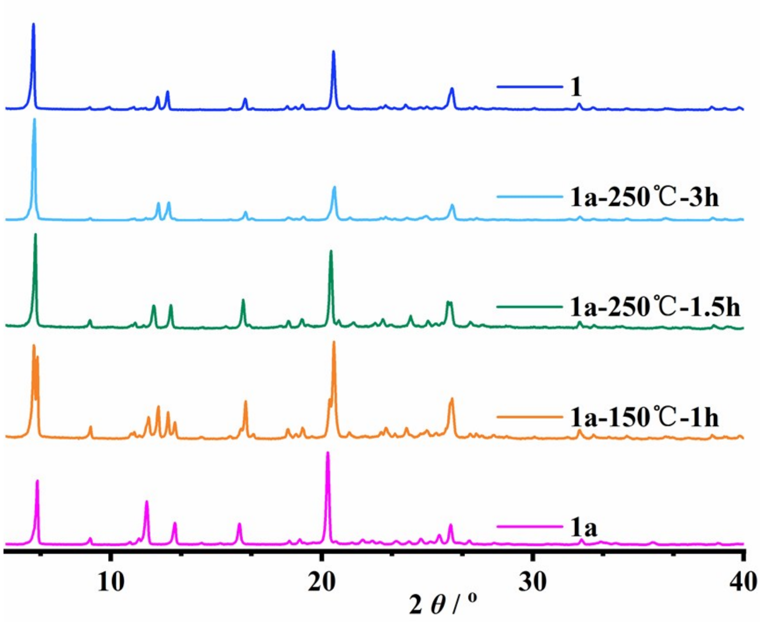

Fig. S4. PXRD patterns of powdered **1a** upon treatment with heat.

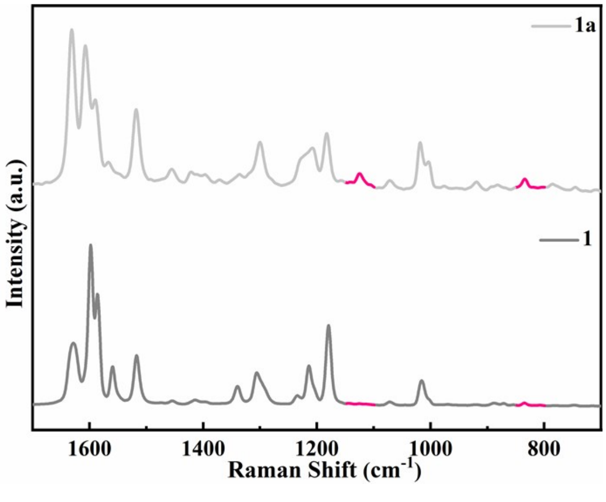

Fig. S5. Raman spectra for the complexes **1** and **1a**.

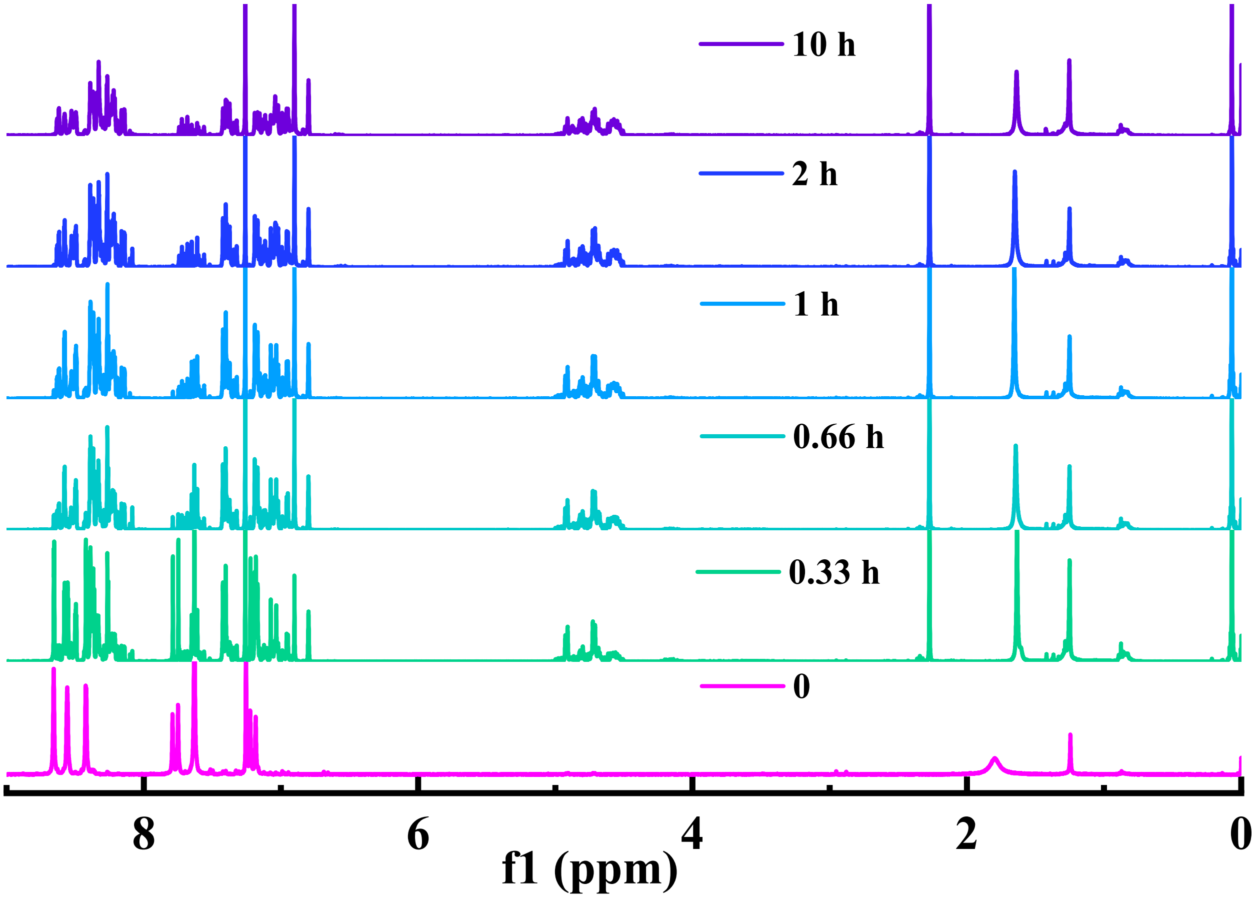

Fig. S6. ^{1}H NMR spectra of **1** in $CDCl_3$ plotted at different UV irradiation times.

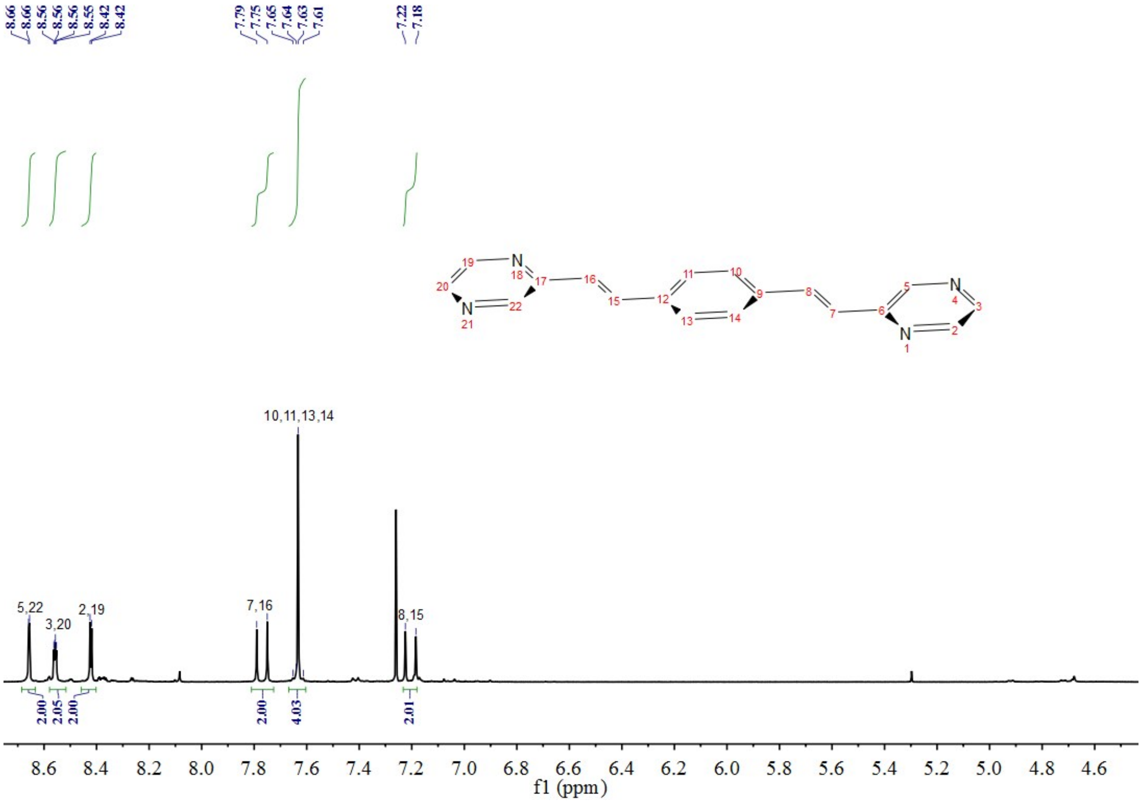

Fig. S7. ^{1}H NMR (400 MHz) of pbzvb.

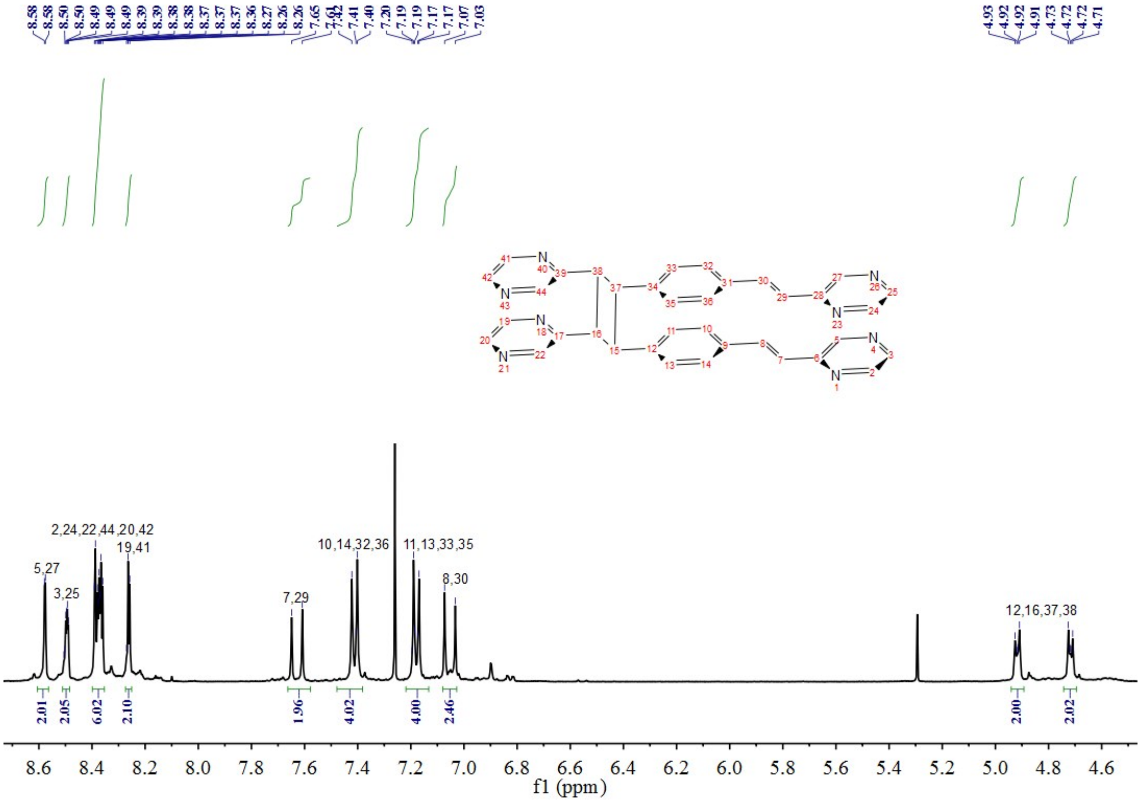

Fig. S8. ^{1}H NMR (400 MHz) of the dimer-I.

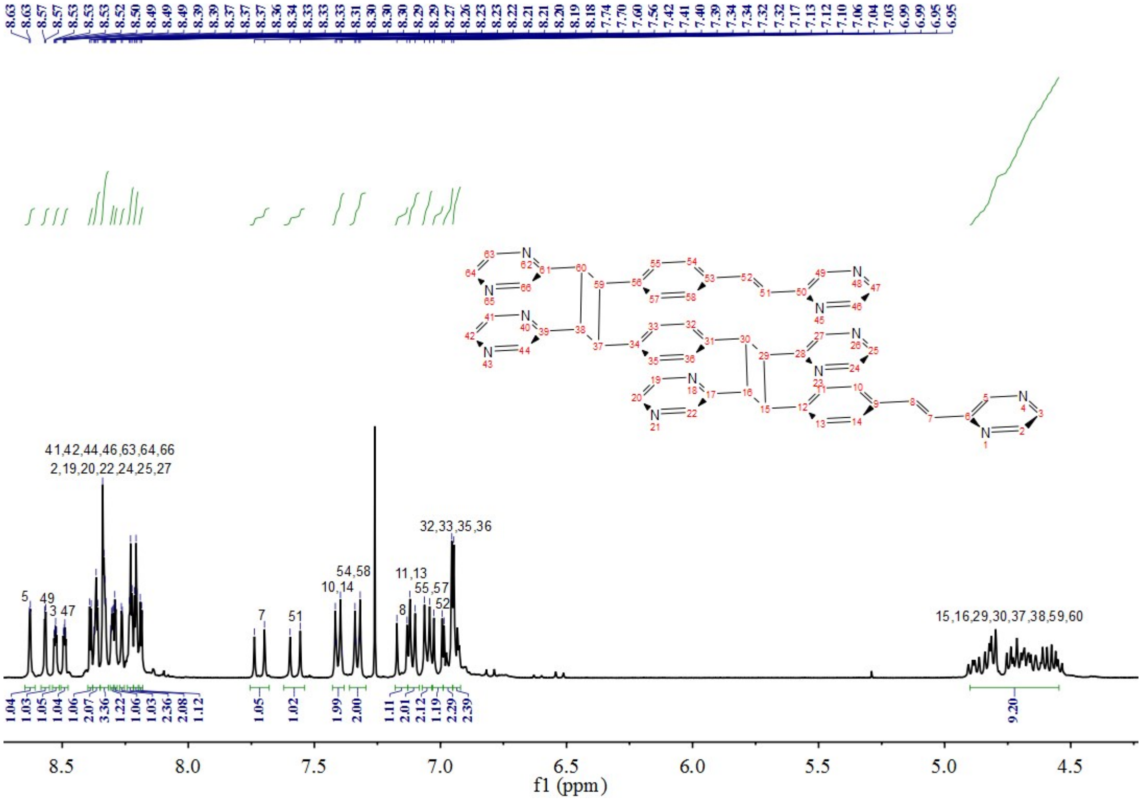

Fig. S9. ^{1}H NMR (400 MHz) of the trimer.

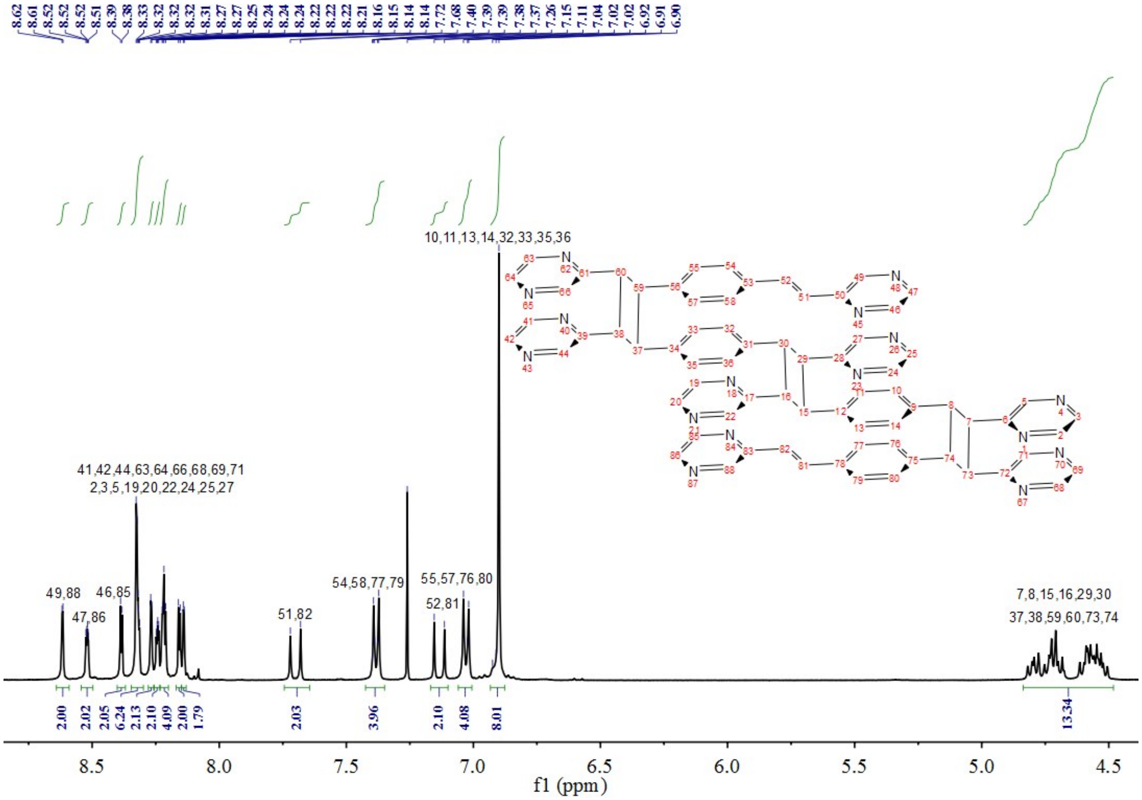

Fig. S10. ^{1}H NMR (400 MHz) of the tetramer.

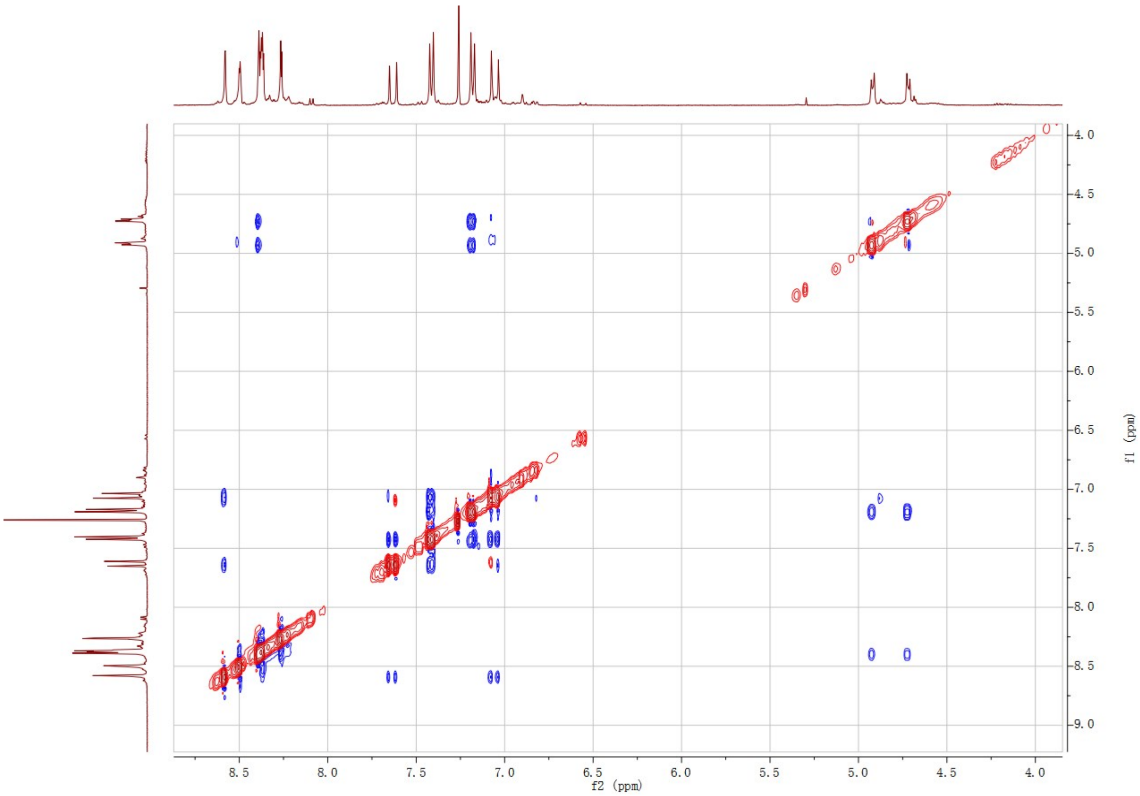

Fig. S11. NOESY of dimer-I.

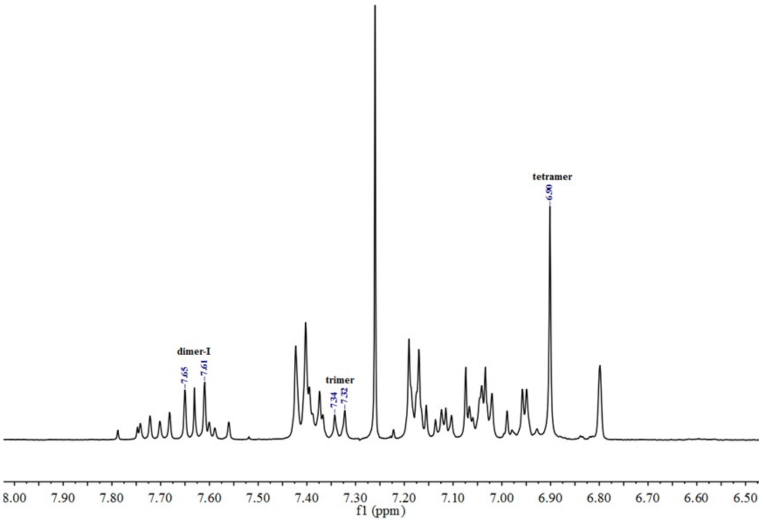

Fig. S12. The characteristic proton peaks of oligomers.

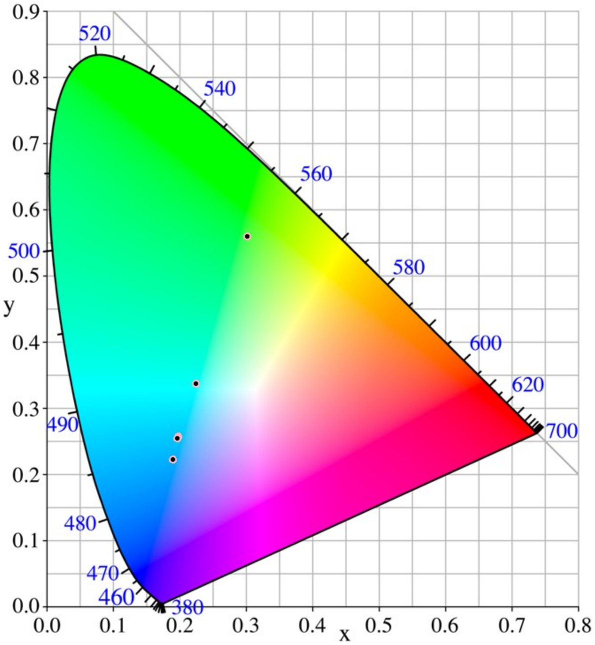

Fig. S13. The trajectory of the CIE color coordinates during the phase transitions of **1** to **1-UV-t**.

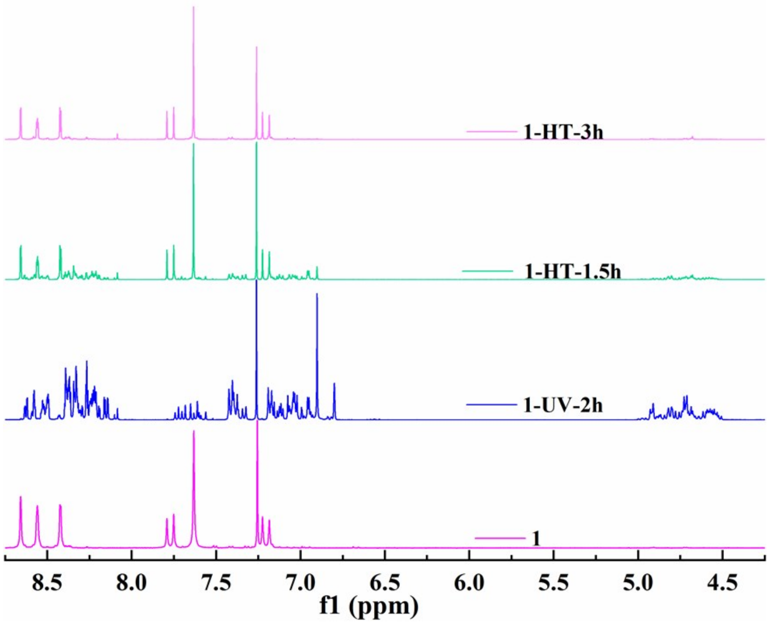

Fig. S14. ^{1}H NMR spectra of **1-UV-2h** upon treatment with heat.

References

S1 M. Hasegawa, Y. Suzuki, F. Suzuki and H. Nakanishi, *J. Polym. Sci.* 1969, **7**, 743.

S2 G. M. Sheldrick, Crystal structure refinement with SHELXL. *Acta Cryst*. 2015, **C71**, 3–8.

S3 G. M. Sheldrick, SHELXT-integrated space-group and crystal-structure determination. *Acta Cryst*. 2015, **A71**, 3–8.

S4 S. Mansab, U. Rafique and M. J. Akhtar, *J. Coord. Chem.*,2018, **71**, 2358.

S5 X. L. Wang, B. Mu, H. Y. Lin and G. C. Liu, *J. Organomet. Chem.*, 2011, **696**, 2313.